RSC Advances

ROYAL SOCIETY OF CHEMISTRY

www.rsc.org/advances

Theoretical Insights into the CO Dimerization and Trimerization on Pt Nanocluster

Yongpeng Yang[a], Ping Cheng[a], Shengli Zhang[b], Shiping Huang[a,*]

[a] State Key Laboratory of Organic-Inorganic Composites, Beijing University of Chemical Technology, Beijing 100029, China

[b] School of Material Science and Technology, Nanjing University of Science and Technology, Nanjing 210094, China

* Corresponding author: Fax: +86-10-64427616 E-mail: huangsp@mail.buct.edu.cn (S. Huang).

ABSTRACT

CO dimerization and trimerization on icosahedral Pt_{55} cluster were investigated using density functional theory. It is found that the products of CO polymerization depend on the different active sites of the metal surface and CO coverage. C_2O_2 can be adsorbed on either two neighboring Pt atoms or one Pt atom, and the former case is preferred. The preference can be ascribed to the stronger interaction between the 8σ orbital of C_2O_2 and 5*d* orbitals of Pt in the former case, and this interaction increases the stability of C_2O_2. Two neighboring adsorbed CO molecules (CO*) can capture one free CO to form a ring-opening CO trimer on the Pt surface. High CO coverage can facilitate the dimerization and trimerization of CO and change the preferred adsorption site of C_2O_2, and highly-coordinated Pt atoms present the superior chemical activity for CO polymerization at high CO coverage. The CO dimerization by two CO* need to overcome a high energy barrier of 1.92 eV, but one CO* can capture one free CO molecule to form the C_2O_2 with overcoming a much lower energy barrier of 0.87 eV. The energy barrier of CO trimerization is 1.14 eV.

1. Introduction

Carbon monoxide hydrogenation to form hydrocarbons (Fischer−Tropsch synthesis) has received much attention both in academia and industry with clean transportation fuels produced from natural gas, coal, and biomass, etc.[1] The process of Fischer−Tropsch (F-T) synthesis is complex and is composed by several elementary steps: chains initiation, chains growth and chains termination. There are several prevalent mechanisms of CO activation and dissociation in the chains initiation. One of the mechanisms is called H-assisted CO dissociation mechanism, where the chemisorbed hydrogen (H*) bonds with chemisorbed CO molecule (CO*) before the CO dissociation.[2-10] The oxygen atoms (O*) in H-assisted CO dissociation are removed as H_2O. Another mechanism is called the carbide mechanism, where CO* dissociates directly on the metal surface to form chemisorbed atomic carbon and oxygen species (C* + O*).[11-13] Then CH_x (x = 1 ~ 3) species are formed by the reaction of C* atom and H* atoms, and O* is removed as CO_2.[1,14-16] In these mechanisms, polymerization of CH_2 leads to the growth of chain.[17,18]

However, Schouten et al. postulated a different mechanism of electrochemical reduction of carbon dioxide to ethylene.[19] In this mechanism, the first step is the formation of a CO dimer. Although no experiment has directly observed the formation of a CO dimer on a metal surface, theoretical calculations on the C-C coupling provide consistent results with available experimental data. Using DFT, it is found that the CO dimer is preferentially adsorbed on Cu(100) rather than on Cu(111), and H^+, Li^+ and Na^+ can facilitate the C-C coupling.[20,21] On the other hand, the mechanism

with a rate-determining CO coupling step reveals that on Cu(100) at low overpotential only C_2 species can be formed, and the formation of C_1 species is hindered.[22] These results coincide with the facts found in the experiments, where the formation of C_2 species on Cu(100) is found easier than on Cu(111), and on Cu(100) at low overpotential only C_2H_4 is observed and CH_4 is not.[23-25] The electrochemical reduction of CO_2 can also occur on the other metal surfaces such as Pt, Cu-Au and Pt-Ru/C.[26,27] Moreover, C_2 species are also found on other metal catalysts such as silver surface in CO_2 electrochemical reduction, although the amounts of C_2 species are small.[28]

In fact, C_2O_2, remaining undetectable even after numerous experimental efforts, is believed to be an intrinsically short-lived molecule. Theoretical calculations indicate C_2O_2 is a triplet, which indeed rapidly dissociates into two CO molecules with a lifetime of 0.5 ns.[29,30] Similarly, neutral $(CO)_n$ ($n > 2$) polymers are also very unstable due to the great tendency toward dissociation into CO molecules.[31-34] In order to increase the stability of $(CO)_n$, it has been demonstrated feasible to change $(CO)_n$ into positively[35,36] or negatively[37] charged oxocarbons, which are more stable than the corresponding neutral ones. Low-valent f-elements with high reduction potentials are found to be applicable to CO coupling. Recently, reductive CO coupling, cyclo-trimerization and cyclo-tetramerization at mild conditions have been exhibited by U(III) complexes.[38-41] Indeed, head-to-head C-C coupling of six CO molecules was observed in the reduction of CO with a ditantalum hydride complex, and the synthesized $(CO)_6$ is stable unless it is exposed in O_2 and H_2O.[31]

In another experiment of CO_2 electroreduction on Cu surfaces, C_3 species were also detected, and the C-C coupling was presented to be involved in the formation of the C_3 species.[42] So in this work, the dimerization, as well as the trimerization, of CO is studied to explore the possibility of C-C bond formation before CO dissociation. Fe and Co are the most common catalysts in F-T synthesis industry, but the CO* dissociates directly on these metal surface.[13] Important experimental and theoretical studies suggest that the activity for CO dissociation is higher for the metals in left-side of the periodic table than that of the metals on the right-hand side, and it decreases from 3d- to 5d-metals.[43,44] The 5d-metals on the right-hand side of the periodic table can be selected to avoid the direct CO dissociation after CO adsorption. Platinum surface may be proper to produce $(CO)_n$ because of its low activity of direct CO dissociation, but the activities for other reactions are very high. For instance, H_2 can be oxidized by O_2 into water on Pt(5 5 7) facet at 298 K.[45] Hydrogenation of unsaturated hydrocarbon compounds, as well as pyrrole, is also easy when selecting platinum as catalyst.[46] Furthermore, the activities relate to the shape and size of metal, e.g. smaller Pt clusters have higher activities for ethylene hydrogenation.[47] High stability of icosahedral Pt_{55} (~ 1 nm) cluster has been demonstrated in many studies.[48,49] Thus, we selected the Pt_{55} cluster to investigate the possible reactions between CO* molecules.

At first, we obtained the most stable geometrical structures of CO, C_2O_2 and C_3O_3 adsorbed on the Pt_{55}. The reaction processes of forming C_2O_2 and C_3O_3 were carried out with the nudged elastic band (NEB) method.[58] Theoretical studies have found CO

coverage can dramatically affect the reaction process. CO dissociation on Rh(1 0 0) is hindered when CO coverage is greater than or equal to 3/12 ML,[50] and the oxidization of CO* by O_2 was facilitated when CO coverage is increased.[51] In order to study CO coverage effect, the most stable geometrical structures of C_2O_2 and C_3O_3 adsorption, as well as the preferred reaction processes of forming corresponding carbon oxides, were researched with high CO coverage taken into account. Finally, we utilized density of states and Mulliken population analysis to investigate the electronic properties of C_2O_2 adsorption.

2. Computational details

Spin-polarized density functional theory (DFT) calculations were carried out using the CP2K code[52] in the Gaussian and plane waves (GPW) formalism.[53] The PBE exchange correlation was employed,[54] as well as the DZVP Molopt local basis sets[55] in combination with Geodecker–Teter–Hutter (GTH) pseudopotentials[56] and a plane wave density cutoff of 300 Ry. The self-consistent field (SCF) convergence criterion was set to be 1.0×10^{-6} Ha and the calculations were performed in a periodic cubic simulation box of $25 \times 25 \times 25$ Å^3, large enough to neglect the interaction between the nanoparticles in periodic images. Geometry optimizations were performed using the Broyden-Fletcher-Goldfarb-Shanno (BFGS) minimization algorithm until the maximum atomic force was less than 4.5×10^{-4} Ha/Bohr.[57] To compute the reaction barrier we used the climbing image nudged elastic band (CI-NEB) method,[58] where the convergence criterion of maximum force on the band was fixed at 2×10^{-3} Ha/Bohr. We chose 8 images for every NEB calculation.

The geometrical structure of icosahedral Pt_{55}, as well as one of the (1 1 1) facets, is shown in Fig. S1 in the Supporting Information. In every facet, there are two different Pt atoms: the corner Pt atom (T1) and the edge Pt atom (T2). The adsorption properties of single CO molecule on Pt_{55} cluster are investigated to confirm the preferred adsorption site, because it is found that some DFT calculations present inconsistent results compared with many experimental studies at low temperature by underestimating CO preference for low-coordination sites on Pt(111).[59] By comparing CO adsorption energies at the six different sites, the adsorption energy decreases in the sequence of T1 > T2 > B1 > B2 > H1 > H2. Namely, the single CO molecule is preferentially adsorbed on the atop site, and the Pt-C bond length is 1.85 Å, which agrees with experimental results fairly well.[59-61]

3. Results and discussion

3.1. Geometrical Structures and Reaction Processes of CO Dimerization and Trimerization on Pt_{55} Cluster

3.1.1 CO Disproportionation and Dimerization on Pt_{55} Cluster without CO Coverage Effect. The geometrical structures of two CO molecules adsorption on Pt_{55} cluster are shown in Fig. 1 (I-IV). As can be seen from Fig. 1, the two CO molecules prefer to occupy two corner Pt atoms and stay away from each other because of repulsive interaction between CO molecules. Various experiments of CO molecules adsorbed on a Pt surface have also confirmed the strong repulsive interaction, which results in the reconstruction of metal surfaces, including the formation of small metallic clusters.[62-65]

We also present other possible structures produced by two CO molecules in Fig. 1 (V-VIII). It is found that two CO molecules can bond with each other by C-C bond to form CO dimer. C_2O_2 can be adsorbed on either two adjacent Pt atoms or one Pt atom, and the former case is preferred. In addition, the energy difference between C_2O_2 adsorption on two edge Pt atoms (structure VI in Fig. 1) and C_2O_2 adsorption on two adjacent corner and edge Pt atoms (structure V in Fig. 1) is very small (0.01 eV). However, the selectivity of adsorption site is relatively high in the cases of C_2O_2 adsorption on one Pt atom, because the energy of C_2O_2 adsorption on the corner site (structure VII in Fig. 1) is lower by 0.23 eV than that of C_2O_2 adsorption on the edge site (structure VIII in Fig. 1).

The reaction processes of C_2O_2 formation and CO disproportionation are investigated. The structure of two CO molecules adsorbed on two adjacent corner and edge Pt atoms is selected as the reactant of all the reactions between CO^* adsorbates. Another reaction path of CO dimerization between one CO^* and one free CO is also considered. In each reaction, we considered several structures of products to find out the most stable products. All the relative energies of structures involved in the reactions are depicted in Fig. 2, and the geometrical parameters of all the minima and transition states are presented in Fig. S2 in the Supporting Information. The disproportionation of CO on the Pt surface is found to be one-step reaction by overcoming a very high energy barrier (4.86 eV), which indicates CO_2 is very unlikely to be generated by CO disproportionation on Pt surface. This result coincides with the conclusion of the experiments of temperature programmed desorption (TPD)

of CO adsorption on the Pt surface.[66,67] In the experiments, little CO_2 produced by disproportionation of CO is detected.

The formation of C_2O_2 adsorbed on one Pt atom by two CO* undergoes two steps. First, the CO adsorbed on the edge Pt atom moves to the B1 site (seen in Fig. S1). During this step, no transition state is observed, and the process is endothermic by 0.45 eV. Then the bridge CO overcomes an energy barrier of 2.76 eV to migrate to the corner site and form the C_2O_2. During the whole reaction process, the energy barrier is 3.21 eV. The CO adsorbed on the corner Pt atom can capture one free CO molecule to form C_2O_2 with overcoming a much lower energy barrier of 0.97 eV.

The formation of C_2O_2 adsorbed on two adjacent corner and edge Pt atoms takes place in only one step, and the energy barrier is 2.25 eV. The C-C distance is 1.60 Å in the product, which is 0.16 Å longer than that in the C_2O_2 adsorbed on one corner Pt atom. However, the Pt-C bonds are shorter by 0.01~0.02 Å in this case.

According to the potential energy surface of neutral C_2O_2 in the previous study, it costs at least 69 kcal/mol (2.99 eV) for two singlet state CO molecules to form isolated C_2O_2.[29] As can be seen from above, when Pt_{55} cluster is involved in the formation of C_2O_2, the necessary energy is dramatically decreased.

3.1.2 CO trimerization on Pt_{55} cluster without High CO Coverage Effect. The structures of three CO molecules adsorbed on Pt_{55} cluster are presented in Fig. 3 (I-IV). Compared with the structure I, the repulsive interaction between the three CO molecules is increased when the adsorbed CO molecules move closely. The main purpose of searching the structures of three CO molecules adsorbed on Pt_{55} cluster is

to confirm whether the C_3O_3 carbonyl compound can form at low CO coverage, and if so, which site C_3O_3 prefers to be adsorbed. Actually, we found three structures containing C_3O_3, shown in V, VI and VII in Fig. 3. The C_3O_3 can be adsorbed either on two adjacent Pt atoms or on corner Pt atom, and it preferably forms on two top edge Pt atoms. However, it failed to find the structure of C_3O_3 adsorbed on one edge Pt atom.

Moreover, in order to verify if C_3O_3 can be formed by two CO* molecules capturing a free CO molecule, we have searched the potential energy surface of the reaction process by the CI-NEB method. Because the preferred adsorption sites of two CO* molecules and C_3O_3 are different, we considered two paths of C_3O_3 formation on two Pt atoms, as presented in Fig. 4. The geometrical parameters of all the minima and transition states involved in the reaction paths are shown in Fig. S3.

As can be seen in Fig. 4, both reactions are one-step processes, and the CO* adsorbed on two adjacent top edge Pt atoms (Path-C1) is better at capturing an additional CO to form C_3O_3 by overcoming a lower energy barrier of 1.13 eV. In Path-C1, the free CO bonds with the two adsorbed CO molecules at the same time. While in the other process, the free CO bonds with the CO molecules adsorbed on the edge site first, then it combines with the corner CO.

On the other hand, isolated C_3O_3 is also very unstable. Using HF, G2, and CBS methods, the symmetry of isolated C_3O_3 (cyclopropanetrione) is D_{3h} with the three C atoms forming an equilateral triangle. The energy of the C_3O_3 triangular molecule is 323~383 kJ/mol (3.45~3.97 eV) higher than that of three CO molecules.[68] However,

no stationary point of C_3O_3 is found using DFT and other high level computational method in previous studies.[33] The free C_3O_3 obtained in this study is a ring-opening compound, and no cyclopropanetrione adsorbed on the Pt_{55} cluster is found. Although C_3O_3 can also be adsorbed at one corner Pt atom, the C-C distance between two terminal C atoms is 2.33 Å, which is too large to form C-C bond. The energy increases by only 0.91 eV when one free CO molecule bonds with two CO* molecules.

3.1.3 CO Disproportionation and Dimerization on Pt_{55} Cluster with High CO Coverage Effect. Due to a strong repulsive interaction between adsorbed CO molecules, the CO coverage should be taken into account while studying the adsorption properties of CO. For this purpose, we have obtained the structure presented in Fig. 5 (I), where 16 CO molecules are adsorbed on the five facets of the Pt_{55} cluster with six CO molecules completely surrounded by the other ten CO molecules. The geometrical structures of C_2O_2 formed by two CO* are presented in Fig. 5 (II-V). Unlike the cluster where only two CO molecules are adsorbed on the Pt_{55}, the preferred adsorption sites of C_2O_2 are two edge Pt atoms when the repulsive interaction between the C_2O_2 and neighboring adsorbed CO is taken into account. What is more, the relative stabilities of all the C_2O_2 isomers are increased by about 0.3 eV. For example, when only two CO molecules are adsorbed, the energy of the cluster where C_2O_2 is adsorbed on one corner Pt atom (structure VII in the Fig. 1) is higher than that of the cluster where two CO molecules are adsorbed on two adjacent edge and corner Pt atoms (structure III in the Fig. 1) by 2.92 eV. However, when the

corner C_2O_2 is surrounded by many CO* molecules, the relative energy is remarkably decreased to 2.58 eV.

Similarly, we still investigated the dimerization and disproportionation processes between the CO* at high CO coverage. Two different dimerization paths and one disproportionation path are performed. The reaction paths are depicted in Fig. 6, and the geometrical parameters of all the minima and transition states involved in the reaction paths are shown in Fig. S4. The three reaction processes change significantly with high CO coverage effect, although the dimerization and disproportionation of CO on two Pt atoms remain to be one-step reaction and the dimerization of CO on one Pt atom is still a two-steps reaction. The active sites of CO dimerization and disproportionation on two atoms are changed into two adjacent edge Pt atoms. On the other hand, all the reactions become easier because of lower energy barriers: the energy barrier of CO disproportionation decreases from 4.86 eV to 4.45 eV, and for the CO dimerization on two edge Pt atoms it decreases from 2.25 eV to 1.92 eV. Besides, no transition state is observed in the first step of C_2O_2 formation on the corner Pt atom, and the energy barrier decreases from 3.21 eV to 2.82 eV in the whole reaction process.

3.1.4 CO dimerization and trimerization with Free CO Molecule Involved at High CO Coverage. Generally, it is found that each surface metal atom can interact with more than one CO molecules, which results in significantly great ratio between the CO* and the surface metal atoms.[65] In this section we will study the adsorption behavior of additional CO when each surface Pt atom has adsorbed one CO molecule.

In addition, the structures discussed in this section are based on the structure where sixteen CO molecules are adsorbed on the five facets of the Pt_{55} cluster. First, the preferred adsorption site of the additional CO is investigated. When the free CO is adsorbed on the B1 site, the adjacent CO adsorbed on the T2 site (seen in the Fig. S1) is found to be forced to migrate to another neighboring B1 site, corresponding to the structure II shown in Fig. 7. Namely, one edge Pt atom attaches two bridge CO molecules, and the adsorption energy of the additional CO in this structure is the largest (1.43 eV) among all the considered cases. The additional CO can be also adsorbed on other sites, including the B2 and hollow sites, without changing the adsorption pattern of neighboring CO.

At the high CO coverage, it is found the free CO can also interact with CO* molecules to form the CO dimer and trimer, as shown in Fig. 7 (IV-IX). For the dimerization between the free CO molecule and CO*, the C_2O_2 prefers to be adsorbed on the edge Pt atom rather than the corner Pt atom, which is contrary to the studies of C_2O_2 adsorption on one Pt atom in the $Pt_{55}(CO)_2$ and $Pt_{55}(CO)_{16}$. For the C_3O_3, the favorite adsorption site is still two edge Pt atoms. It should be emphasized that the C_3O_3 can also be adsorbed on one edge Pt atom, as shown in Fig. 7 (VIII), which is not observed without the CO coverage effect. Meanwhile, the C_3O_3 prefers to be adsorbed on one edge Pt atom rather than one corner Pt atom.

The processes of the free CO molecule reacting with CO* to form CO polymers are illustrated in Fig. 8, and the adsorption process of the free CO molecule to the B2 site is also presented. The geometrical parameters of all the minima and transition states

involved in the reaction paths are shown in Fig. S5. It is observed that the free CO molecule can be easily adsorbed at the B2 site by overcoming an energy barrier of 0.32 eV (Path-E in Fig. 8), although each of the Pt atoms near the adsorption site has adsorbed one CO molecule. In terms of the calculated results of NEB, the CO molecule adsorbed at the B2 site cannot directly bond with two adjacent CO molecules to form the C_3O_3. In Path-C′, the free CO molecule migrates to two neighboring CO molecules adsorbed on two edge Pt atoms to form the C_3O_3. The energy barrier of the C_3O_3 formation is 1.14 eV, which is decreased by 0.22 eV compared with the C_3O_3 formation without the high CO coverage effect. Furthermore, the mobility of this newly formed C_3O_3 is also observed: the C_3O_3 adsorbed on two edge Pt atoms can be adsorbed on one edge Pt atom by overcoming an energy barrier of 1.25 eV, and the two C-C bonds are shortened to 1.56 Å. In the whole reaction process of forming the C_3O_3 adsorbed on one edge Pt atom, the energy barrier is 2.01 eV. The formation of C_2O_2 on one edge Pt atom is also found to be slightly easier with overcoming an energy barrier of 0.87 eV, which is the lowest energy barrier among all the considered reaction process of CO polymer formation.

3.2. Electronic Properties of C_2O_2 Adsorption on Pt_{55} cluster

The electronic structure such as density of states (DOS) can present deep insight into the interaction between the adsorbate and metal surface. In this section we use the DOS to explain how the C_2O_2 is adsorbed on the Pt_{55} cluster with or without the CO coverage effect.

In Fig. 9, we plot the projected density of states (PDOS) of the C_2O_2 and the Pt atoms before and after the C_2O_2 adsorption. The relevant molecular orbitals of one free C_2O_2 molecule are plotted in Fig. S6 in the Supporting Information. The two uppermost occupied orbitals of the free C_2O_2 are two singly-occupied 3π orbitals, represented as $3\pi^{(*)}$. Because the ground state of the free C_2O_2 molecule is a triplet, we plot its DOS of spin up and spin down at the same time. While the DOS of spin up and spin down are the same not only for the adsorbed C_2O_2 but also for the Pt atoms after C_2O_2 adsorption, we used the spin polarized calculation method. Thus we plotted only the DOS of spin up for the adsorbed C_2O_2 and the bonding Pt atoms.

As can be obtained from Fig. 9-(b), when the C_2O_2 is adsorbed on the two neighboring corner and edge Pt atoms, the two carbon atoms re-hybridize from *sp* to sp^2. What is noteworthy is that only the 8σ orbital shifts to lower energy by about 0.3 eV compared with the free C_2O_2, but the other orbitals shift to higher energy. For example, the 7σ orbital shifts to higher energy by as much as 2.0 eV. The shift to higher energy arises from the elongated C-C bond length (1.61 Å), which weakens the interaction between the two C atoms. For the Pt atoms connected with the C_2O_2, their *d* orbitals interact with the 8σ orbital of C_2O_2, resulting in the shift to lower energy of these orbitals. The 8σ orbital dominates the interaction between the C_2O_2 and Pt atoms. On the other hand, in according to the newly formed peaks of the DOS of Pt at -12.0, -6.0, -5.0 and 2.0 eV, other orbitals of the C_2O_2, including 7σ, 9σ, 1π, 2π and 3π, are also found to participate in the interaction between the adsorbate and the metal surface. The molecular orbitals of the C_2O_2 after adsorption on two Pt atoms are

exhibited in Fig. 10. As can be seen from the Fig. 10, the π orbitals in z-axis are broken after C_2O_2 adsorption. Since the 8σ and 9σ orbital are anti-bonding orbitals in the C_2O_2, the interactions between the two orbitals and the Pt cluster increase the stability of the C_2O_2 with donating the electron from the 8σ and 9σ orbitals to the metal. The interactions of the π orbitals of C_2O_2 with the Pt cluster decrease the stability of C_2O_2 because of the electron donation from the 1π and 2π orbitals to the empty metal orbitals and the electron back donation from the Pt cluster to the empty $3\pi^*$ orbitals. However, the 8σ orbital dominates the electron transfer due to its strong interaction with the Pt cluster. Thus the C_2O_2 transfers 0.13 electrons to the Pt_{55} cluster in the light of the Mulliken population analysis.

In Fig. 9(c), when the C_2O_2 is adsorbed on one corner Pt atoms, the two carbon atoms also re-hybridize from *sp* to sp^2. All the orbitals except the 8σ shift to lower energy compared with C_2O_2 adsorbed on two Pt atoms. There are two reasons leading to this fact. The first one is that the C-C bond length is 1.44 Å, which is much shorter, resulting in the enhancement of the interaction between the two carbon atoms. The second one is that the interactions between the orbitals of C_2O_2 and the metal orbitals also are strengthened, as can be seen from that all the bonding orbitals of the Pt atom dramatically shift to lower energy. But the orbital overlap between the 8σ and the metal orbitals is not increased, and the energy of 8σ is 0.3eV higher. The bonding orbitals of the C_2O_2 adsorbed on one corner Pt atom are depicted in Fig. S7 in the Supporting Information. It is worth noting that the interaction between the empty $3\pi^*$ of C_2O_2 and the *d* orbitals of Pt is relatively strong due to part of $3\pi^*$ state

dramatically shifting to lower energy near the Femi level, leading to more electrons transferred from Pt atom to empty $3\pi^*$ orbital.

When the CO coverage effect is taken into account, all the bonding interactions between the C_2O_2 and Pt are weakened, because the intensities of the peaks below -5.0 eV are weakened especially for the Pt, as shown in the Fig. 9(d, e). The adsorption of CO can change the geometrical and electronic properties of the Pt cluster. The repulsive interaction between adsorbed CO elongates the bond length of neighboring Pt atoms, and every CO molecule donates as many as 0.3 electrons to the Pt cluster. The high CO coverage weakens the adsorption of C_2O_2 on the Pt_{55} cluster, and the adsorption of CO is also weakened as found in previous studies.[61,65]

4. Conclusions

In summary, the adsorption properties of CO, C_2O_2 and C_3O_3 on the icosahedral Pt_{55} cluster were investigated. It is found the CO prefers to be adsorbed at the corner site without the effect of CO coverage, while the high CO coverage leads to the CO migration from the top site to the bridge site. The CO can dimerize to form a C-C bond not only on two Pt atoms but also on one Pt atom. In the former case, the C-C bond length is 1.60 Å, and in the latter case it is 1.44 Å. The dimer prefers to be adsorbed on two Pt atoms rather than one Pt atom. The preference can be ascribed to the stronger interaction between the 8σ orbital of C_2O_2 and the 5*d* orbitals of Pt for the C_2O_2 adsorbed on two Pt atoms, and this interaction increases the stability of C_2O_2. But for the C_2O_2 adsorbed on one Pt atom, the interaction between the $3\pi^*$ orbital of the C_2O_2 and the 5*d* orbitals of Pt is stronger, resulting in the decrease of the C_2O_2

stability. The C_3O_3 also prefers to be adsorbed on two Pt atoms rather than one Pt atom. The high CO coverage can weaken the adsorption strength of the CO adsorption, which is beneficial for the CO polymerization, although the adsorption strength of CO polymers is also weakened. When the CO coverage is increased to 1 ML, the energy barrier of the CO dimerization by two CO* is decreased from 2.26 eV to 1.92 eV, which is still much too high. However, the CO* can capture one free CO molecule to form the C_2O_2 and C_3O_3 by overcoming much lower energy barriers. At the high CO coverage, the energy barrier of the CO dimerization by one CO* and one free CO molecule is decreased from 0.97 eV to 0.87 eV, and the energy barrier of the CO trimerization by two one CO* and one free CO molecule is decreased from 1.36 eV to 1.14 eV. Thus, the CO polymerization between CO* and free CO should be considered especially when the CO coverage or CO pressure is high. In this study, we have investigated the static properties of the CO dimerization and trimerization on the Pt cluster. In order to gain more accurate results about the stabilities of CO dimer and trimer, pressure and temperature should be considered, and that is what we will do in our next study.

Acknowledgments

This work is supported by the National Natural Science Foundation of China (Grant No. 21376013)

References

1 F. Fischer and H. Tropsch, *Brennst. Chem.*, 1926, **7**, 97-116.

2 H. Pichler and H. Schulz, *Chem. Ing. Tech.*, 1970, **42**, 1162-1174.

3 X. Dai and C. Yu, *J. Nat. Gas Chem.*, 2008, **17**, 365-368.

4 M. Ojeda, R. Nabar, A. U. Nilekar, A. Ishikawa, M. Mavrikakis and E. Iglesia, *J. Catal.*, 2010, **272**, 287-297.

5 F. M. Hoffmann and J. L. Robbins, *J. Electron Spectrosc. Relat. Phenom.*, 1987, **45**, 421–428.

6 C. F. Huo, J. Ren, Y. W. Li, J. Wang and H. Jiao, *J. Catal.*, 2007, **249**,174-184.

7 O. R. Inderwildi, S. J. Jenkins and D. A. King, *J. Phys. Chem. C*, 2008, **112**, 1305-1307.

8 G. A. Morgan, Jr., D. C. Sorescu, T. Zubkov and J. T. Yates, Jr., *J. Phys. Chem. B*, 2004, **108**, 3614-3624.

9 O. R. Inderwildi, S. J. Jenkins and D. A. King, *J. Am. Chem. Soc.*, 2007, **129**, 1751-1759.

10 O. R. Inderwildi, S. J. Jenkins and D. A. King, *Angew. Chem. Int. Ed.*, 2008, **47**, 5253-5255.

11 T. Zubkov, G. A. Morgan, Jr., J. T. Yates, Jr., O. Kühlert, M. Lisowski, R. Schillinger, D. Fick and H. J. Jänsch, *Surf. Sci.*, 2003, **526**, 57-71.

12 C. Y. Fan, H. P. Bonzel and K. Jacobi, *J. Chem. Phys.*, 2003, **118**, 9773- 9782.

13 Q. Ge and M. Neurock, *J. Phys. Chem. B*, 2006, **110**, 15368-15380.

14 M. M. Kappes and R. H. Staley, *J. Am. Chem. Soc.*, 1981, **103**, 1286-1287.

15 M. Araki and V. Ponec, *J. Catal.*, 1976, **44**, 439-448.

16 C. S. Kellner and A. T. Bell, *J. Catal.*, 1981, **67**, 175-185.

17 D. S. Santilli and D. G. Castner, *Energy Fuels*, 1989, **3**, 8-15.

18 V. V. Ordomsky, B. Legras, K. Cheng, S. Paul and A. Y. Khodakov, *Catal. Sci. Technol.*, 2015, **5**, 1433-1437.

19 K. J. P. Schouten, Y. Kwon, C. J. M. van der Ham, Z. Qin and M. T. M. Koper, *Chem. Sci.*, 2011, **2**, 1902-1909.

20 J. H. Montoya, A. A. Peterson and J. K. Nørskov, *ChemCatChem*, 2013, **5**, 737-742.

21 J. H. Montoya, C. Shi, K. Chan and J. K. Nørskov, *J. Phys. Chem. Lett.*, 2015, **6**, 2032 −2037.

22 F. Calle-Vallejo and M. T. M. Koper, *Angew. Chem.*, 2013, **125**, 7423 –7426.

23 M. Gattrell, N. Gupta and A. Co, *J. Electroanal. Chem.*, 2006, **594**, 1-19.

24 K. J. P. Schouten, E. P. Gallent and M. T. M. Koper, *ACS Catal.*, 2013, **3**, 1292-1295.

25 K. J. P. Schouten, Z. Qin, E. P. Gallent and M. T. M. Koper, *J. Am. Chem. Soc.*, 2012, **134**, 9864-9867.

26 F. Jia, X. Yu, L. Zhang, *J. Power Sources* 2014, **252**, 85-89.

27 S. Shironita, K. Karasuda, K. Sato, M. Umeda, *J. Power Sources* 2013, **240**, 404-410.

28 T. Hatsukade, K. P. Kuhl, E. R. Cave, D. N. Abram and T. F. Jaramillo, *Phys. Chem. Chem. Phys.*, 2014, **16**, 13814-13819.

29 D. Schröder, C. Heinemann, H. Schwarz, J. N. Harvey, S. Dua, S. J. Blanksby and J. H. Bowie, *Chem. Eur. J.*, 1998, **4**, 2550-2557.

30 G. P. Raine, H. F. Schaefer, III and R. C. Haddon, *J. Am. Chem. Soc.*, 1983, **105**, 194-198.

31 T. Watanabe, Y. Ishida, T. Matsuo and H. Kawaguchi, *J. Am. Chem. Soc.*, 2009, **131**, 3474-3475.

32 R. B. Wyrwas and C. C. Jarrold, *J. Am. Chem. Soc.*, 2006, **128**, 13688-13689.

33 X. Bao, X. Zhou, C. F. Lovitt, A. Venkatraman, D. A. Hrovat, R. Gleiter, R. Hoffmann and W. T. Borden, *J. Am. Chem. Soc.*, 2012, **134**, 10259-10270.

34 H. Jiao and H. S. Wu, *J. Org. Chem.*, 2003, **68**, 1475-1479.

35 S. Schlemmer, A. Luca, J. Glosik and D. Gerlich, *J. Chem. Phys.*, 2002, **116**, 4508-4516.

36 K. Hiraoka, T. Mori and S. Yamabe, *J. Chem. Phys.*, 1991, **94**, 2697-2703.

37 R. M. Morris and K. J. Klabunde, *J. Am. Chem. Soc.*, 1983, **105**, 2633-2639.

38 S. M. Mansell, N. Kaltsoyannis and P. L. Arnold, *J. Am. Chem. Soc.*, 2011, **133**, 9036-9051.

39 O. P. Lam and K. Meyer, *Angew. Chem. Int. Ed.*, 2011, **50**, 9542-9544.

40 O. T. Summerscales, F. G. N. Cloke, P. B. Hitchcock, J. C. Green and N. Hazari, *Science*, 2006, **311**, 829-831.

41 O. T. Summerscales, F. G. N. Cloke, P. B. Hitchcock, J. C. Green and N. Hazari, *J. Am. Chem. Soc.*, 2006, **128**, 9602-9603.

42 K. P. Kuhl, E. R. Cave, D. N. Abram and T. F. Jaramillo, *Energy Environ. Sci.*, 2012, **5**, 7050–7059.

43 S. S. Sung and R. Hoffmann, *J. Am. Chem. Soc.*, 1985, **107**, 578-584.

44 B. Hammer and J. K. Nørskov, *Adv. Catal.*, 2000, **45**, 71-129.

45 Z. Zhu, G. Melaet, S. Axnanda, S. Alayoglu, Z. Liu, M. Salmeron and G. A. Somorjai, *J. Am. Chem. Soc.*, 2013, **135**, 12560-12563.

46 C. K. Tsung, J. N. Kuhn, W. Huang, C. Aliaga, L. I. Hung, G. A. Somorjai and P. Yang, *J. Am. Chem. Soc.*, 2009, **131**, 5816-5822.

47 H. Song, R. M. Rioux, J. D. Hoefelmeyer, R. Komor, K. Niesz, M. Grass, P. Yang and G. A. Somorjai, *J. Am. Chem. Soc.*, 2006, **128**, 3027-3037.

48 J. H. Ryu, S. S. Han, D. H. Kim, G. Henkelman and H. M. Lee, *ACS Nano*, 2011, **5**, 8515-8522.

49 E. Aprà and A. Fortunelli, *J. Phys. Chem. A*, 2003, **107**, 2934-2942.

50 X. Zhao, R. Zhang, L. Ling and B. Wang, *Appl. Surf. Sci.*, 2014, **320**, 681-688.

51 S. Dobrin, *Phys. Chem. Chem. Phys.*, 2012, **14**, 12122-12129.

52 J. VandeVondele, M. Krack, F. Mohamed, M. Parrinello, T. Chassaing and J. Hutter, *Comput. Phys. Commun.*, 2005, **167**, 103-128.

53 G. Lippert, J. Hutter and M. Parrinello, *Mol. Phys.*, 1997, **92**, 477-488.

54 J. P. Perdew, K. Burke and Y. Wang, *Phys. Rev. B*, 1996, **54**, 16533-16539.

55 J. VandeVondele and J. Hutter, *J. Chem. Phys.*, 2007, **127**, 114105.

56 S. Goedecker, M. Teter and J. Hutter, *Phys. Rev. B*, 1996, **54**, 1703-1710.

57 B. G. Pfrommer, M. Côté, S. G. Louie and M. L. Cohen, *J. Comput. Phys.*, 1997, **131**, 233-240.

58 G. Henkelman, B. P. Uberuaga and H. Jonsson, *J. Chem. Phys.*, 2000, **113**, 9901-9904.

59 P. J. Feibelman, B. Hammer, J. K. Nørskov, F. Wagner, M. Scheffler, R. Stumpf, R. Watwe and J. Dumesic, *J. Phys. Chem. B*, 2001, **105**, 4018-4025.

60 P. Gruene, A. Fielicke, G. Meijer and D. M. Rayner, *Phys. Chem. Chem. Phys.*, 2008, **10**, 6144-6149.

61 M. Gajdoš, A. Eichler and J. Hafner, *J. Phys.: Condens. Matter*, 2004, **16**, 1141-1164.

62 R. Brako and D. Šokčević, *Surf. Sci.*, 1998, **401**, L388-L394.

63 F. Tao, S. Dag, L. W. Wang, Z. Liu, D. R. Butcher, M. Salmeron and G. A. Somorjai, *Nano Lett.*, 2009, **9**, 2167-2171.

64 F. Tao, S. Dag, L. W. Wang, Z. Liu, D. R. Butcher, H. Bluhm, M. Salmeron and G. A. Somorjai, *Science*, 2010, **327**, 850-853.

65 B. T. Loveless, C. Buda, M. Neurock and E. Iglesia, *J. Am. Chem. Soc.*, 2013, **135**, 6107-6121.

66 K. Foger and J. R. Anderson, *Appl. Surf. Sci.*, 1979, **2**, 335-351.

67 T. Yamamoto, T. Shido, S. Inagaki, Y. Fukushima and M. Ichikawa, *J. Phys. Chem. B*, 1998, **102**, 3866-3875.

68 G. Corkran and D. W. Ball, *J. Mol. Struct. (Theochem)*, 2004, **668**, 171-178.

Figure Caption

Fig. 1. Geometrical structures of two CO molecules adsorption and dimerization on Pt_{55} cluster.

Fig. 2. Geometric structures and relative energies of all the minima and transition states involved in the reactions of CO dimerization on two neighboring corner and edge Pt atoms (Path-A1), CO dimerization on one corner Pt atom (Path-A2 and Path-A3), and CO disproportionation on two neighboring corner and edge Pt atoms (Path-B).

Fig. 3. Geometrical structures of three CO molecules adsorption and trimerization on the Pt_{55} cluster.

Fig. 4. Geometric structures and relative energies of all the minima and transition states involved in the reactions of CO trimerization on two edge Pt atoms (Path-C1) and CO trimerization on two neighboring corner and edge Pt atoms (Path-C2).

Fig. 5. Geometrical structures of sixteen CO molecules adsorbed on five facets in the Pt_{55} cluster.

Fig. 6. Geometric structures and relative energies of all the minima and transition states involved in the reactions of CO dimerization on two neighboring corner and edge Pt atoms (Path-A1′), CO dimerization on one corner Pt atom (Path-A2′), and CO disproportionation on two neighboring corner and edge Pt atoms (Path-B′) with high CO coverage effect.

Fig. 7. Geometrical structures of seventeen CO molecules adsorption on five facets of the Pt_{55} cluster. The energy of the structure (I) containing one free CO molecule is set

at 0.00 eV.

Fig. 8. Geometric structures and relative energies of all the minima and transition states involved in the reactions of an additional free CO adsorbed at the B1 site (Path-D), CO dimerization between a free CO molecule and a corner CO* on one corner Pt atom (Path-E), and CO trimerization on two edge Pt atoms (Path-C1′) with high CO coverage effect.

Fig. 9. The PDOS of free C_2O_2 (a) and adsorbed C_2O_2 on two neighboring corner and edge Pt atoms (b), on one corner Pt atom (c), on two neighboring corner and edge Pt atoms in $Pt_{55}(CO)_{16}$ (d), and on one corner Pt atom in $Pt_{55}(CO)_{17}$ (e). The right side is the PDOS of Pt atoms before adsorption and Pt atoms adjacent to C_2O_2, respectively.The Fermi level is set at 0.00 eV.

Fig. 10. 7σ (a), 8σ (b), 9σ (c), 1π (d,e), 2π (f,g) and $3\pi^{(*)}$ (h,i) orbitals of C_2O_2 when C_2O_2 is adsorbed on two Pt atoms.

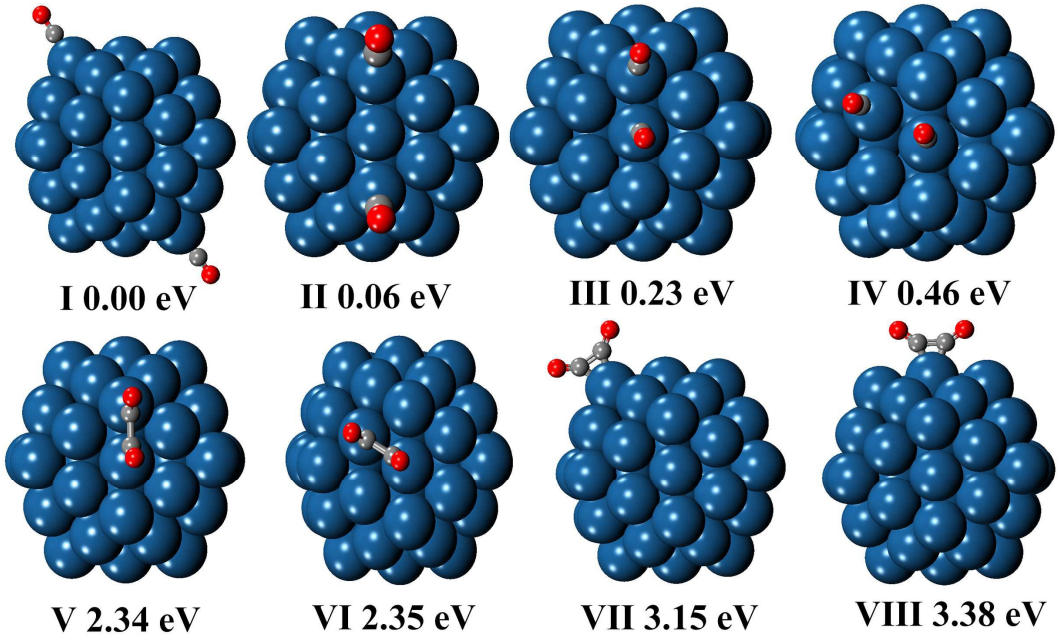

Fig. 1. Geometrical structures of two CO molecules adsorption and dimerization on Pt_{55} cluster.

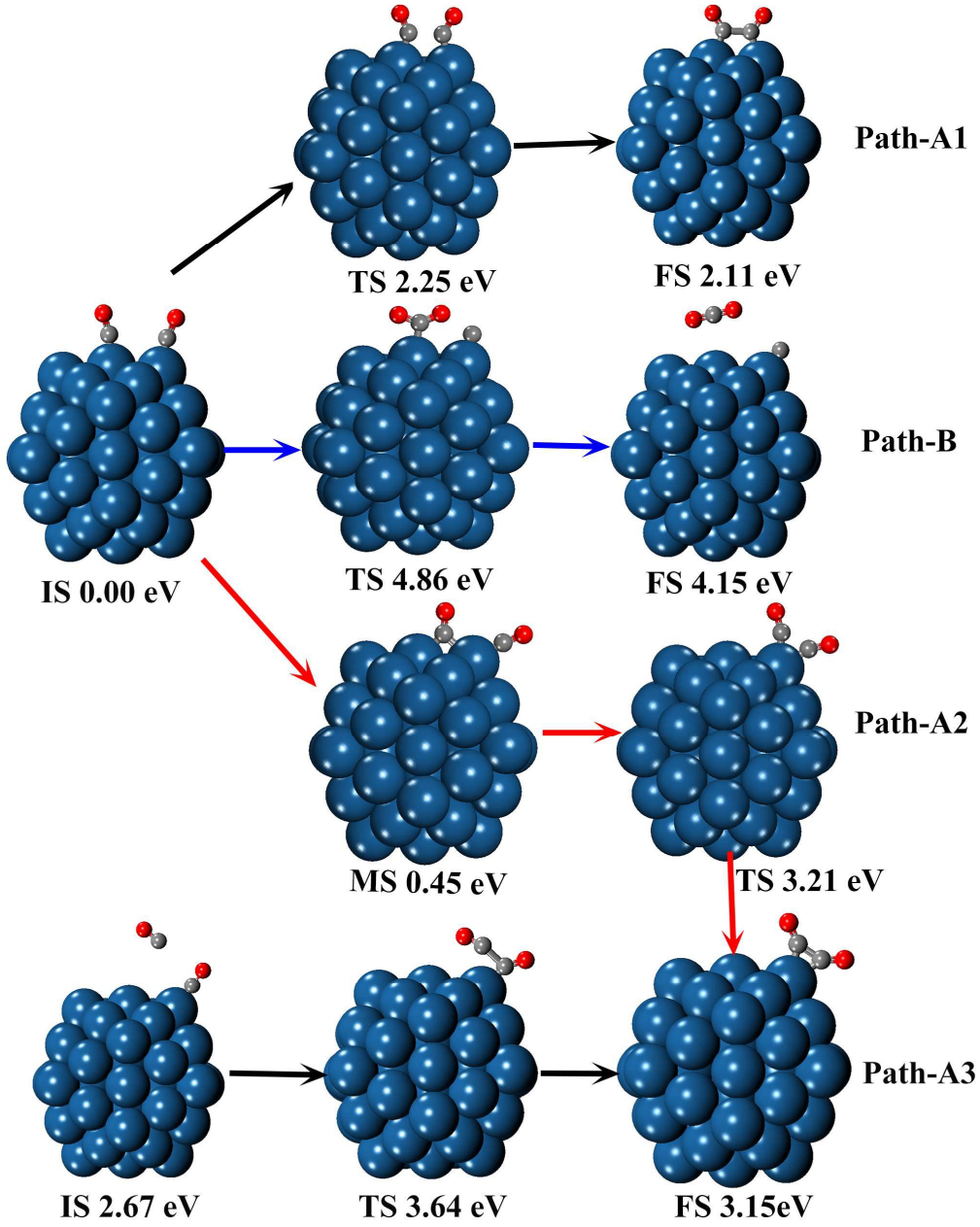

Fig. 2. Geometric structures and relative energies of all the minima and transition states involved in the reactions of CO dimerization on two neighboring corner and edge Pt atoms (Path-A1), CO dimerization on one corner Pt atom (Path-A2 and Path-A3), and CO disproportionation on two neighboring corner and edge Pt atoms (Path-B).The IS, MS, TS, and FS represent the initial state, metastable state, transition state and final state, respectively.

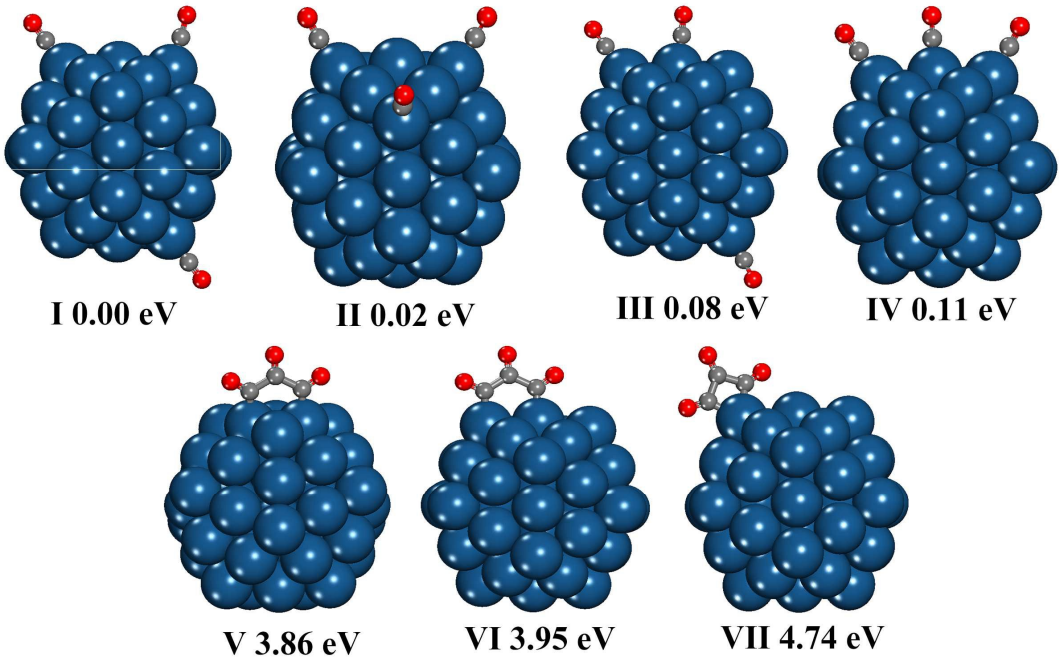

Fig. 3. Geometrical structures of three CO molecules adsorption and trimerization on the Pt_{55} cluster.

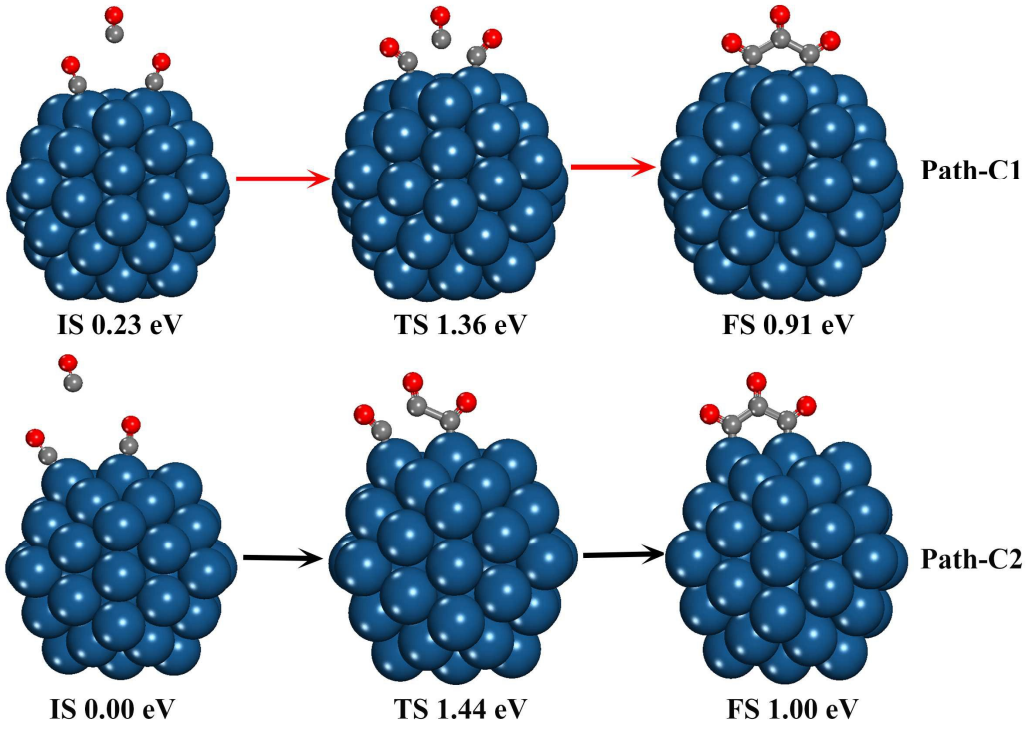

Fig. 4. Geometric structures and relative energies of all the minima and transition states involved in the reactions of CO trimerization on two edge Pt atoms (Path-C1) and CO trimerization on two neighboring corner and edge Pt atoms (Path-C2). The IS, TS, and FS represent the initial state, transition state and final state, respectively.

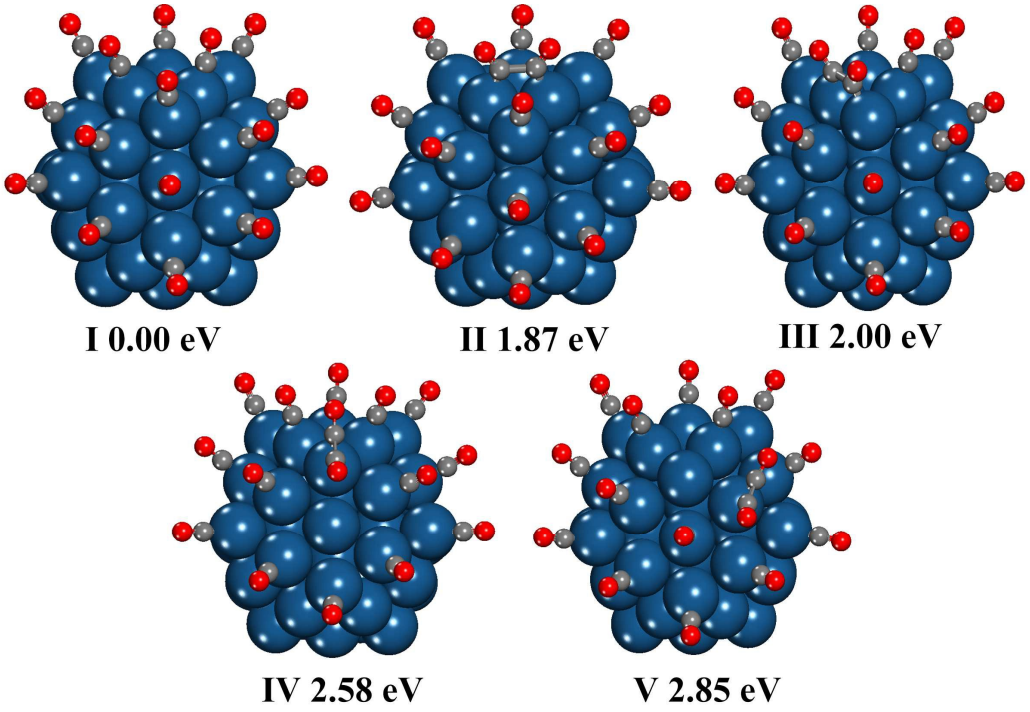

Fig. 5. Geometrical structures of sixteen CO molecules adsorbed on five facets in Pt_{55} cluster.

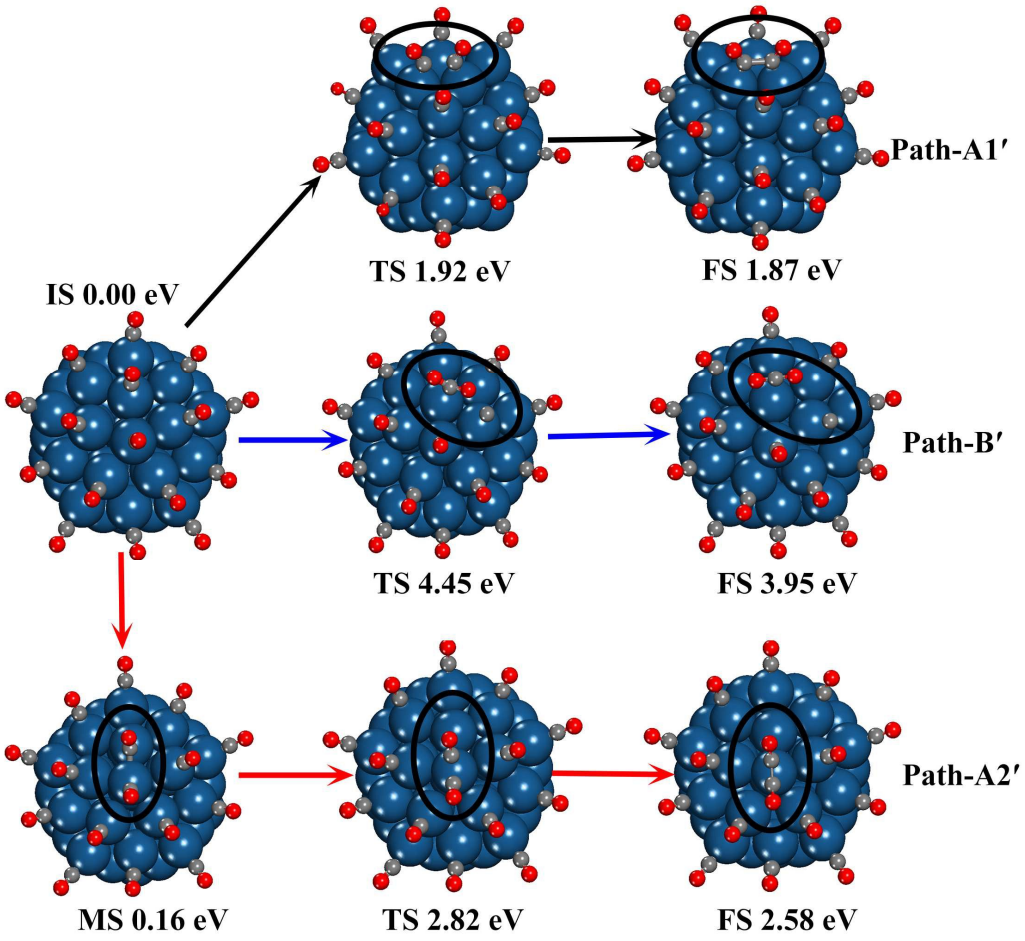

Fig. 6. Geometric structures and relative energies of all the minima and transition states involved in the reactions of CO dimerization on two neighboring corner and edge Pt atoms (Path-A1′), CO dimerization on one corner Pt atom (Path-A2′), and CO disproportionation on two neighboring corner and edge Pt atoms (Path-B′) with high CO coverage effect. The IS, MS, TS, and FS represent the initial state, metastable state, transition state and final state, respectively.

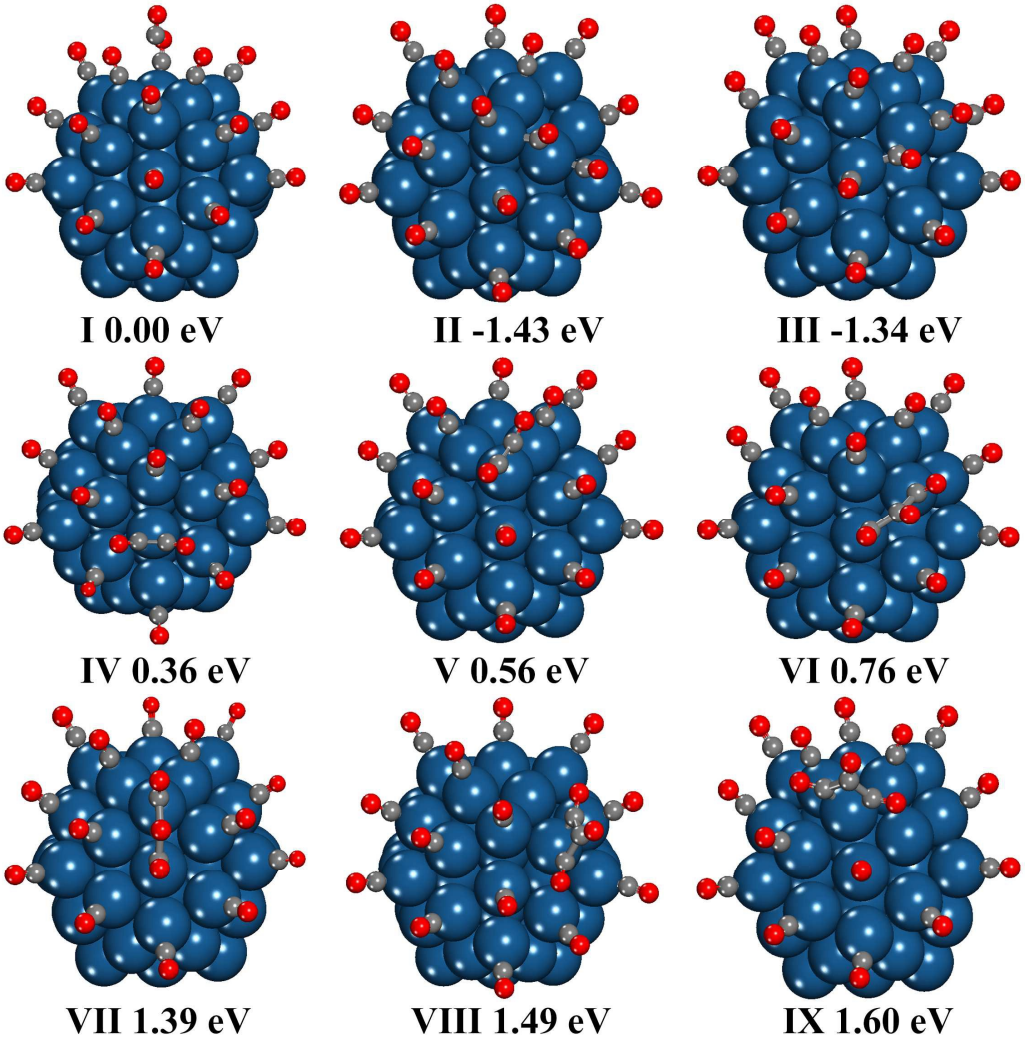

Fig. 7. Geometrical structures of seventeen CO molecules adsorption on five facets of the Pt_{55} cluster. The energy of the structure (I) containing one free CO molecule is set at 0.00 eV.

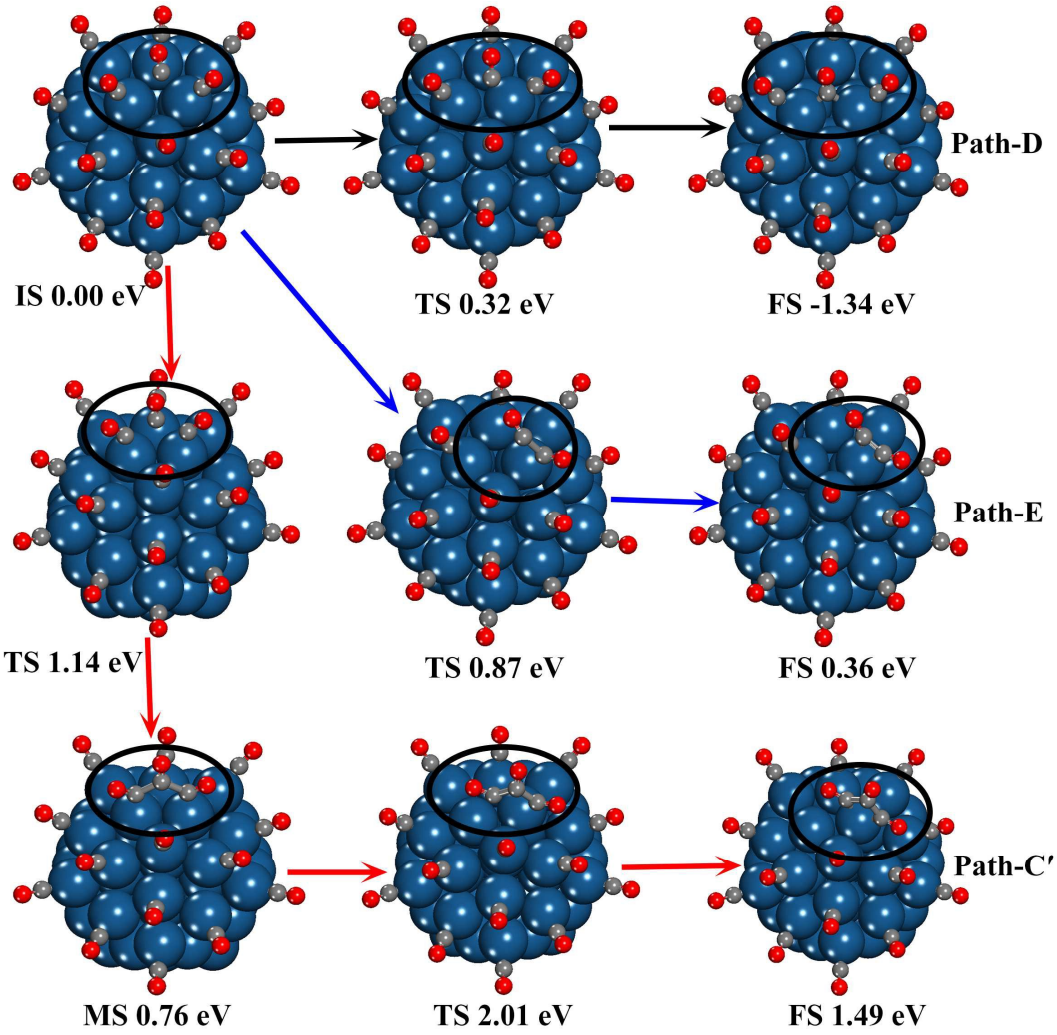

Fig. 8. Geometric structures and relative energies of all the minima and transition states involved in the reactions of an additional free CO adsorbed at the B1 site (Path-D), CO dimerization between a free CO molecule and a corner CO* on one corner Pt atom (Path-E), and CO trimerization on two edge Pt atoms (Path-C1′) with high CO coverage effect. The IS, MS, TS, and FS represent the initial state, metastable state, transition state and final state, respectively.

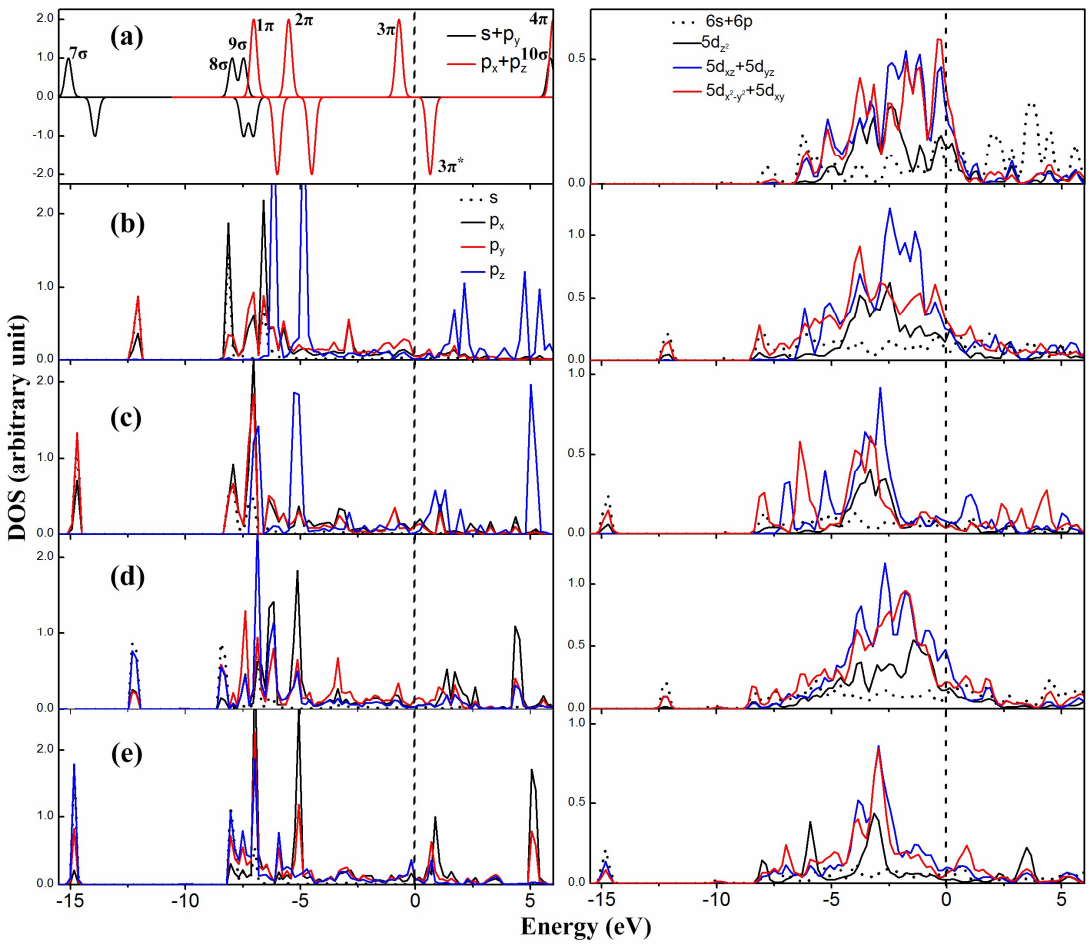

Fig. 9. The PDOS of free C_2O_2 (a) and adsorbed C_2O_2 on two neighboring corner and edge Pt atoms (b), on one corner Pt atom (c), on two neighboring corner and edge Pt atoms in $Pt_{55}(CO)_{16}$ (d), and on one corner Pt atom in $Pt_{55}(CO)_{17}$ (e). The right side is the PDOS of Pt atoms before adsorption and Pt atoms adjacent to C_2O_2, respectively.The Fermi level is set at 0.00 eV.

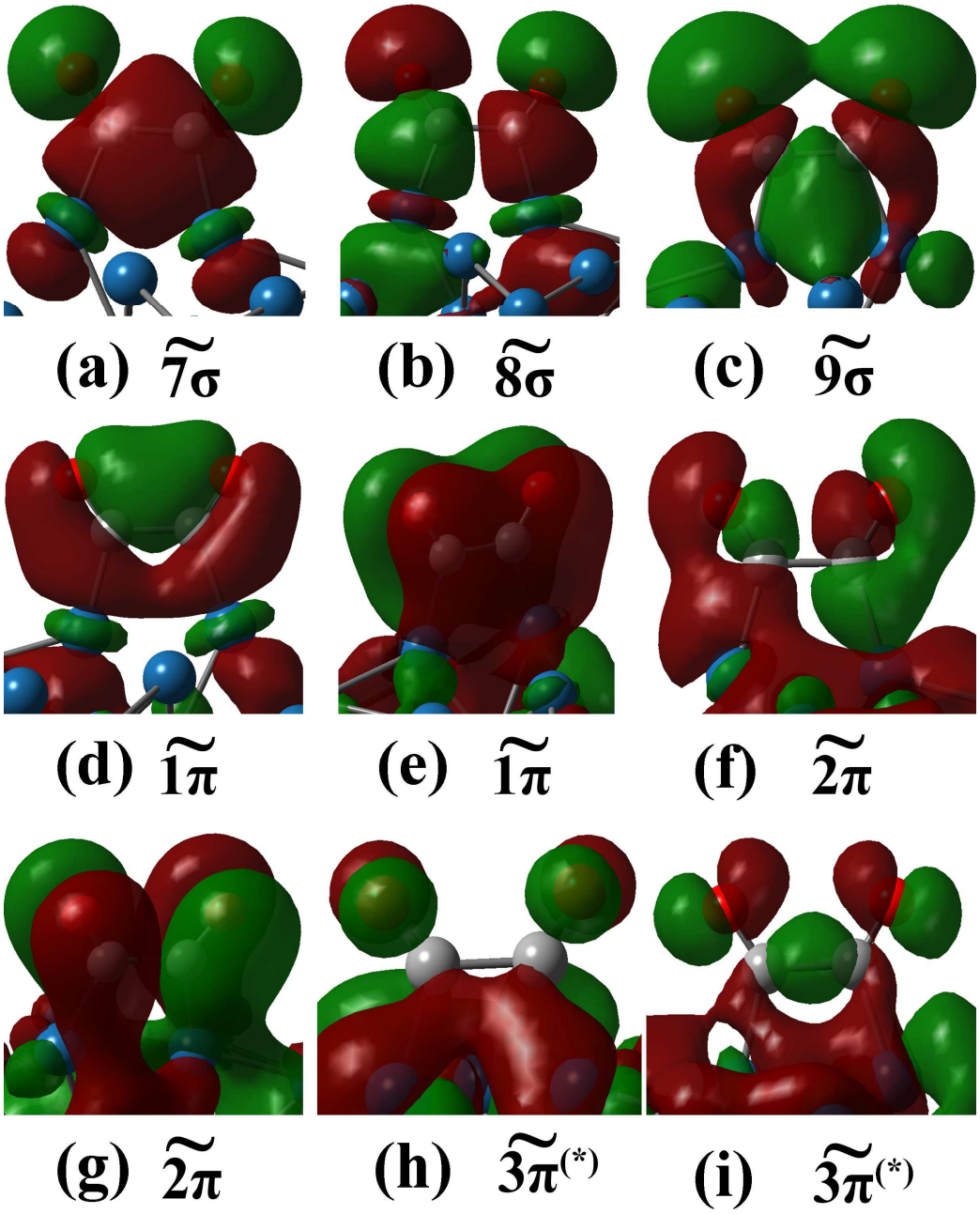

Fig. 10. 7σ (a), 8σ (b), 9σ (c), 1π (d,e), 2π (f,g) and $3\pi^{(*)}$ (h,i) orbitals of C_2O_2 when C_2O_2 is adsorbed on two Pt atoms.